12. M. Kürster, *Astron. Astrophys.* **274**, 851 (1993).
13. F. M. Walter, D. M. Gibson, G. S. Basri, *Astrophys. J.* **267**, 665 (1983).
14. N. E. White, R. A. Shafer, K. Horne, A. N. Parmar, J. L. Culhane, *ibid.* **350**, 776 (1990).
15. R. Ottmann, J. H. M. M. Schmitt, M. Kürster, *ibid.* **413**, 710 (1993).
16. N. E. White, J. L. Culhane, A. N. Parmar, M. A. Sweeney, *Mon. Not. R. Astron. Soc.* **227**, 545 (1987).
17. J. L. Culhane, N. E. White, R. A. Shafer, A. N. Parmar, *ibid.* **243**, 424 (1990).
18. B. M. Haisch, J. H. M. M. Schmitt, M. Rodonó, D. M. Gibson, *Astron. Astrophys.* **230**, 419 (1990).
19. N. E. White *et al.*, *Astrophys. J.* **301**, 262 (1986).
20. P. L. Bornmann and L. D. Matheson, *Astron. Astrophys.* **231**, 525 (1990).
21. J. Tomkin and D. M. Popper, *Astron. J.* **91**, 1428 (1986).
22. J. H. M. M. Schmitt *et al.*, *Astrophys. J.* **351**, 492 (1990).
23. J. Trümper *et al.*, *Nature* **349**, 579 (1991).
24. J. H. M. M. Schmitt, in *Proceedings of the G. S. Vaiana Memorial Symposium "Advances in Stellar and Solar Coronal Physics,"* J. L. Linsky and S. Serio, Eds. (Kluwer, Dordrecht, Netherlands, in press).
25. S. Kirkpatrick, C. D. Gelatt Jr., M. P. Vecchi, *Science* **220**, 671 (1983).
26. D. G. Bounds, *Nature* **329**, 215 (1987).
27. W. Jeffrey and B. Rosner, *Astrophys. J.* **310**, 473 (1986).
28. R. Rosner, W. H. Tucker, G. S. Vaiana, *ibid.* **220**, 643 (1978).

6 May 1993; accepted 11 August 1993

Confinement of Electrons to Quantum Corrals on a Metal Surface

M. F. Crommie, C. P. Lutz, D. M. Eigler

A method for confining electrons to artificial structures at the nanometer lengthscale is presented. Surface state electrons on a copper(111) surface were confined to closed structures (corrals) defined by barriers built from iron adatoms. The barriers were assembled by individually positioning iron adatoms with the tip of a 4-kelvin scanning tunneling microscope (STM). A circular corral of radius 71.3 Å was constructed in this way out of 48 iron adatoms. Tunneling spectroscopy performed inside of the corral revealed a series of discrete resonances, providing evidence for size quantization. STM images show that the corral's interior local density of states is dominated by the eigenstate density expected for an electron trapped in a round two-dimensional box.

When electrons are confined to lengthscales approaching the de Broglie wavelength, their behavior is dominated by quantum mechanical effects. Here we report the construction and characterization of structures for confining electrons to this lengthscale. The walls of these "quantum corrals" are built from Fe adatoms which are individually positioned on the Cu(111) surface by means of a scanning tunneling microscope (STM). These adatom structures confine surface state electrons laterally because of strong scattering that occurs between surface state electrons and the Fe adatoms. The surface state electrons are confined in the direction perpendicular to the surface because of intrinsic energetic barriers that exist in that direction (*1*). Since similar surface states exist on all noble metals (*2*–*6*), we expect that the behavior reported here is not unique to Cu.

One quality that separates these new structures from quantum dots formed from semiconductor heterostructures is that the quantum states of the corrals may be resolved spatially as well as spectroscopically. Analysis of the spatial and spectroscopic properties of a ring of 48 Fe adatoms reveals that this corral is well described by solutions to Schrödinger's equation for a particle in a hard-wall enclosure. Despite this agreement, however, the details of the confinement mechanism are not completely understood.

The experiments were performed with an STM contained in ultrahigh vacuum and cooled to 4 K (*7*, *8*). Operation at low temperature provided the stability, cleanliness, and absence of thermal diffusion of adsorbates required for this experiment. The single-crystal Cu sample was prepared by repeated cycles of Ar ion sputtering and annealing. The Auger-clean sample was then cooled to 4 K and dosed with a calibrated electron-beam Fe evaporator (0.005 monolayer coverages were typical). The convention used here is that the bias across the tunnel junction (V) is the voltage of the sample measured with respect to the tip. dI/dV spectra were measured through lock-in detection of the ac tunnel current driven by a 205-Hz, 10-mV (rms) signal added to the junction bias. All STM images were acquired in the constant current mode with a polycrystalline tungsten wire as the STM tip.

The confinement property of the Fe adatom structures derives from the scattering of surface state electrons by Fe adatoms. The results of this scattering can be seen in Fig. 1A, which shows a 130 Å × 130 Å STM image of a single Fe adatom on the Cu(111) surface (acquired with a bias of 0.02 V). The local density of states (LDOS) at E_F surrounding the adatom is marked by a circular standing wave pattern caused by the interference of incident and scattered surface state electrons (*5*). Figure 1B shows a cross sectional slice of the adatom image, more clearly displaying the 15 Å period oscillations.

If the Fe adatom is modeled as a cylindrically symmetric scattering potential, then the change in surface LDOS around the adatom is determined by the partial wave phase shifts of the scattered surface state electrons. At low energies, the change in LDOS far from the Fe adatom can be approximated as (*5*)

$$\Delta\mathrm{LDOS}(\rho) \propto \frac{1}{k\rho}\left(\cos^2\left(k\rho - \frac{\pi}{4} + \delta_0\right) - \cos^2\left(k\rho - \frac{\pi}{4}\right)\right) \quad (1)$$

where $k = (2m^*E/\hbar^2)^{1/2}$. Here δ_0 is the phase shift of the $l = 0$ scattered wave, m^* is the effective mass of a surface state electron (0.38 m_e) (*2*, *5*, *9*), and E is the energy measured from the surface state band-edge. By fitting Eq. 1 to our linescan data (as shown in Fig. 1B), we find that the Fe scattering strength at E_F can be characterized by an $l = 0$ phase shift of $\delta_0 = -80° \pm 5°$, which indicates strong scattering.

The strong scattering of surface state electrons by Fe adatoms suggests that they would be good building blocks for constructing microscopic electron confinement structures. In order to test this idea, we used the adatom "sliding" process (*7*, *10*) to position individual Fe adatoms into orderly structures on the Cu(111) surface (bias parameters during the slide process were 0.01 volt and 5×10^{-8} amp). Figure 2A shows an STM image of 48 Fe atoms that have been positioned into a ring. This image was taken at a bias of 0.01 V. The ring has a mean radius of 71.3 Å, and the spacing between neighboring Fe atoms varies from 8.8 Å to 10.2 Å (*11*). A striking feature of Fig. 2A is the strong modulation of the LDOS inside of the Fe ring. Figure 2B shows a linescan taken through the center of the ring.

A standard method for characterizing an electronic system is to measure its density of states via tunneling spectroscopy (*12*). With an STM this is done by measuring the differential conductivity (dI/dV) of the tunnel junction (*13*). Figure 3 shows dI/dV spectra measured with the STM tip centered over different points on the surface. The top curve shows the spectrum measured with the tip held over a Cu terrace about 1000 Å away (laterally) from the Fe ring. This spectrum is relatively featureless, with the dominant characteristic being a

IBM Research Division, Almaden Research Center, 650 Harry Road, San Jose, CA 95120–6099.

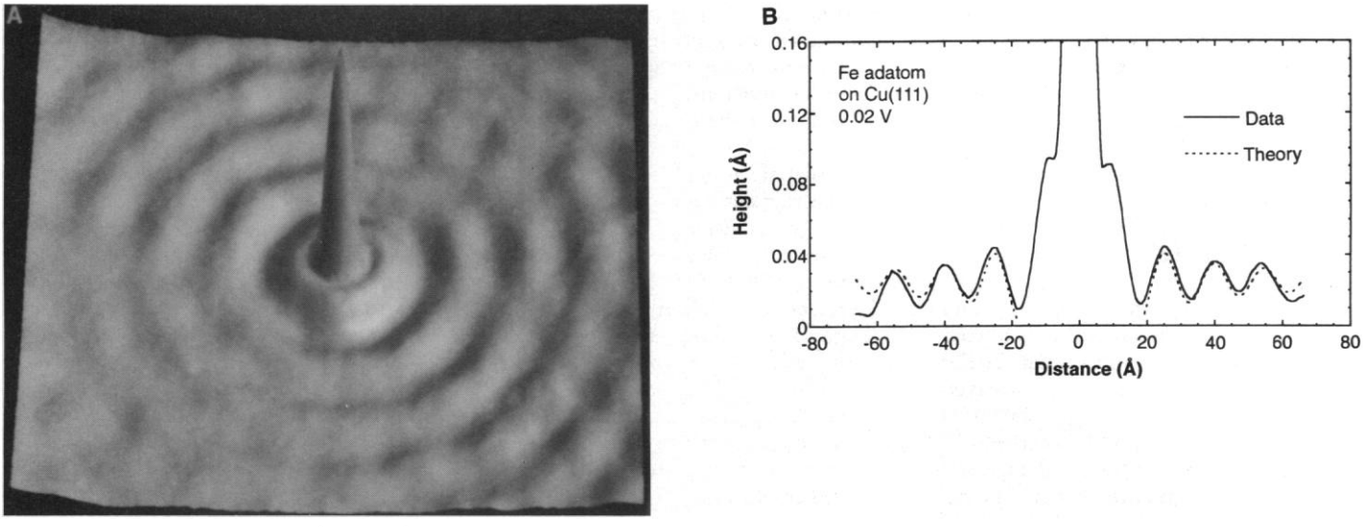

Fig. 1. (**A**) Constant current 130 Å × 130 Å image of an Fe adatom on the Cu(111) surface (V = 0.02 volt, I = 1.0 nA). The apparent height of the adatom is ~0.9 Å. The concentric rings surrounding the Fe adatom are standing waves due to the scattering of surface state electrons with the Fe adatom. (**B**) Solid line: average of three cross sections taken through the center of the Fe adatom image in (A). Dashed line: fit of Eq. 1 to the cross section (the data was fit only up to 18 Å from the center of the adatom).

sharp drop in dI/dV at the surface state band edge 0.44 eV below E_F. [There is also a slight peak around zero bias which we believe is due to the tip electronic structure (*14*).] Similar spectra were seen at other points on the Cu terraces with this tip. The second curve in Fig. 3 shows a dI/dV spectrum measured with the STM tip held over the center of the ring (with the same tip and tunneling parameters as before). This spectrum is dominated by a series of sharp peaks. The peaks have a roughly Lorentzian shape, and widths ranging from ~35 mV to ~100 mV. The width of the peak centered at zero bias was found to be insensitive to variations in tunnel current over two orders of magnitude. The third curve in Fig. 3 shows the dI/dV spectrum measured with the STM tip positioned 9 Å away (laterally) from the center of the ring (the tunneling parameters and tip remained unchanged). Here the spectrum reveals the existence of additional peaks in the surface LDOS. The locations of four new peaks are marked in the figure.

Measurements of dI/dV spectra were complicated by adatom motion and variability of the STM tip. During the ~1 minute required to take each of the ring spectra of Fig. 3, typically 20% of the border atoms would move one or two lattice spacings, even though the tip was located over the center of the ring, "far" from the border atoms. At the low bias voltages used for imaging, the Fe adatoms did not move. The adatom motion caused negligible changes in spectra for $V \leq 0$, but peaks at $V > 0$ suffered some broadening (*15*). Use of different STM tips had the main effect of introducing a variable linear offset to the spectra. Measured peak widths and energies, however, were not sensitive to the STM tip. For example, three identical 48-atom rings constructed at different locations on the surface and measured with different tips all yielded very similar results.

We can understand the main features of the 48-atom ring in a straightforward manner. Since the surface state electrons are strongly scattered by Fe adatoms, we model the ring as a continuous hard wall barrier, a

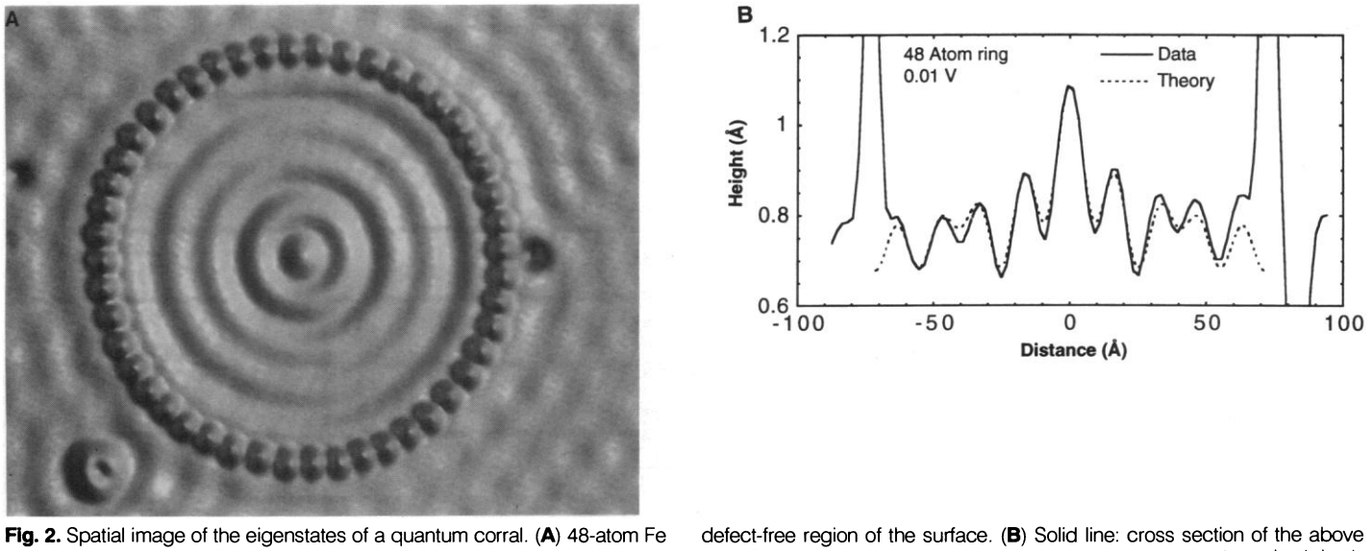

Fig. 2. Spatial image of the eigenstates of a quantum corral. (**A**) 48-atom Fe ring constructed on the Cu(111) surface (V = 0.01 volt, I = 1.0 nA). Average diameter of ring (atom center to atom center) is 142.6 Å. The ring encloses a defect-free region of the surface. (**B**) Solid line: cross section of the above data. Dashed line: fit to cross section using a linear combination of $|5,0\rangle$, $|4,2\rangle$, and $|2,7\rangle$ eigenstate densities.

round "box" containing the 2D surface state electrons. The eigenstates inside of a 2D box of radius r can be written (*16*) as $\psi_{n,l}(\rho,\phi) \propto J_l(k_{n,l}\rho)e^{il\phi}$, with wavenumber $k_{n,l} = \chi_{n,l}/r$ and energy $E_{n,l} = \hbar^2 k^2_{n,l}/(2m^*)$. Here l is the angular momentum quantum number of an electron in the box, J_l is the l^{th} order Bessel function, and $\chi_{n,l}$ is the n^{th} zero crossing of $J_l(\chi)$. States with quantum numbers (n,l) will be referred to as $|n,l\rangle$.

Figure 4 shows the low-lying theoretical eigenenergies for the $|n,0\rangle$, $|n,1\rangle$, and $|n,2\rangle$ states inside of a round box having the same radius as the ring in Fig. 2. For comparison, the eigenenergies derived from the spectra of Fig. 3 are shown as horizontal lines in Fig. 4 (theoretical energies are referenced to the band edge and experimental energies are obtained by fitting Lorentzians to the spectral peaks). The spectroscopic peaks observed in the LDOS at the center of the ring are seen to lie very close to the theoretical $|n,0\rangle$ eigenenergies. This is expected from the model, since all non-zero angular momentum states have a node at the origin. The four new peaks seen in the LDOS when the tip is 9 Å off-center lie extremely close to the theoretical $|n,1\rangle$ eigenenergies. This is also expected, since $|n,1\rangle$ states should dominate any new spectral features seen in the LDOS just away from the origin (higher angular momentum states have less amplitude near the origin due to the centrifugal barrier).

The spatial variation of the LDOS inside of the Fe ring can be understood by examining the distribution of round-box eigenstates near E_F. Figure 4 shows that the energies of the $|5,0\rangle$ and $|4,2\rangle$ eigenstates fall very close to E_F. A study of the $l>2$ eigenstates (not shown in Fig. 4) reveals that the only other eigenstate lying within 25 mV of E_F is the $|2,7\rangle$ state. As a result, we expect the LDOS at E_F inside the ring to be dominated by these states. This can be tested by fitting the experimentally measured cross section in Fig. 2B to a linear combination of $J_0^2(k_{5,0}\,\rho)$, $J_2^2(k_{4,2}\,\rho)$, and $J_7^2(k_{2,7}\rho)$. Figure 2B shows that this procedure gives a good fit to the linescan data (*17*).

Our data differ from the ideal behavior of a particle in a hard-wall box in that the measured spectral lines have finite width and the energies of the lines deviate from the ideal predicted values. The measured linewidths are narrow compared to photoemission measurements of free Cu(111) surface state electrons (9), but correspond to a lifetime of only $\sim 3 \times 10^{-14}$ at E_F (for comparison, a free surface state electron at E_F travels a distance equal to the ring's diameter in $\sim 2 \times 10^{-14}$ s). Some possible broadening mechanisms are transmission past the boundary atoms (along the surface), decay into the bulk (9), and inelastic scattering. These mechanisms may also contribute to the discrepancy between the measured peak energies and the predictions of the hard-wall model. Another possible contribution to that discrepancy is the resonant electronic structure of the individual Fe adatoms. This will modify the confinement properties of the quantum corral by adding an energy dependence to the boundary condition on the wavefunction of the enclosed electrons.

In conclusion, we have discovered a method for shaping the spatial distribution of surface state electrons at the atomic scale. This ability opens up possibilities for studying the properties of confined electrons, as well as the interaction of surface state electrons with adsorbates. One can conceive of a number of electron containment structures [such as polygons, stadia (*18*), anti-dot arrays, and waveguides] whose interior wavefunctions are now accessible to spatial mapping.

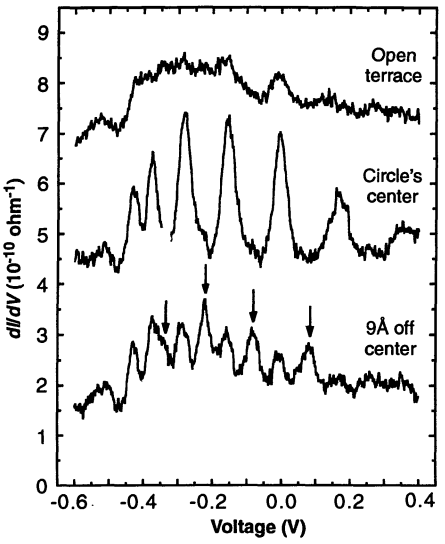

Fig. 3. Spectra (*dI/dV*) taken with the STM tip 1000 Å away from 48-atom Fe ring ("open terrace"), at the center of the Fe ring, and 9 Å away from the center of the ring. The tip was kept stationary during spectrum acquisition by opening the feedback loop during each voltage ramp. The lateral drift was negligible. The dc tunnel current at +0.4 volt was 0.05 nA for all three spectra. The center spectrum has been shifted vertically by 2.9×10^{-10} ohm^{-1} and the open terrace spectrum has been shifted by 5.4×10^{-10} ohm^{-1}. The *dI/dV* spectra give an energy resolved measure of the local density of states at different points inside of the ring. New states appearing when the tip is moved 9 Å from the ring's center are shown with arrows.

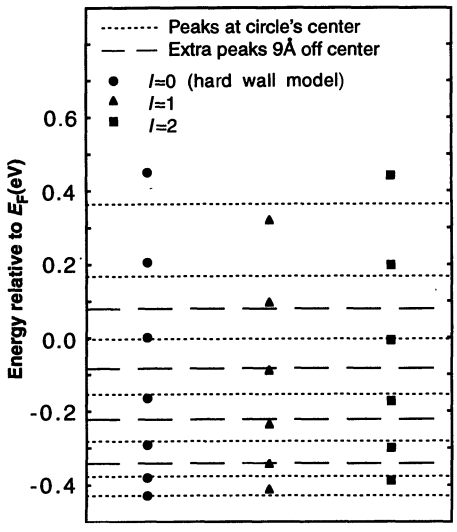

Fig. 4. Theoretical eigenenergies for l = 0, 1, and 2 states of "hard wall" circular box (solid symbols) compared to experimental energies (dashed lines) extracted from *dI/dV* spectra of Fig. 3.

REFERENCES AND NOTES

1. A. Zangwill, *Physics at Surfaces* (Cambridge University Press, Cambridge, 1988).
2. P. O. Gartland and B. J. Slagsvold, *Phys. Rev. B* **12**, 4047 (1975).
3. P. Heimann, H. Neddermeyer, H. F. Roloff, *J. Phys. C* **10**, L17 (1977).
4. M. P. Everson, R. C. Jaklevic, W. Shen, *J. Vac. Sci. Technol. A* **8**, 3662 (1990).
5. M. F. Crommie, C. P. Lutz, D. M. Eigler, *Nature* **363**, 524 (1993).
6. Y. Hasegawa and P. Avouris, *Phys. Rev. Lett.* **71**, 1071 (1992).
7. D. M. Eigler and E. K. Schweizer, *Nature* **344**, 524 (1990).
8. D. M. Eigler, P. S. Weiss, E. K. Schweizer, N. D. Lang, *Phys. Rev. Lett.* **66**, 1189 (1991).
9. S. D. Kevan, *ibid.* **50**, 526 (1983).
10. J. A. Stroscio and D. M. Eigler, *Science* **254**, 1319 (1991).
11. We observed the Fe adatoms to bind to only one position per Cu(111) surface unit cell, presumably a threefold hollow. In contrast, on the Pt(111) surface we observed Fe adatoms to bind to two sites per surface unit cell, presumably the threefold hollows (*14*).
12. E. L. Wolf, *Principles of Electron Tunneling Spectroscopy* (Oxford University Press, New York, 1989).
13. N. D. Lang, *Phys. Rev. B* **34**, 5947 (1986).
14. M. F. Crommie, C. P. Lutz, D. M. Eigler, *Phys. Rev. B* **48**, 2851 (1993).
15. For the present experiments the adatom motion proved to be a nuisance. We anticipate that this problem may be avoided by choosing an adatom with greater corrugation energy. The mechanism of adatom motion is not known to us.
16. R. Haberman, *Elementary Applied Partial Differential Equations* (Prentice-Hall, Englewood Cliffs, NJ, 1983).
17. Here we assume that variations in tip height are small enough that the barrier penetration factor can be linearized. To justify this we checked that exponentiating the data with an experimentally derived decay constant of 1.84 Å^{-1} leads to only negligible differences.
18. E. J. Heller, *Phys. Rev. Lett.* **53**, 1515 (1984).

19. We gratefully acknowledge useful discussions with E. J. Heller, R. Nesbit, S. C. Zhang, B. A. Jones, and M. S. Sherwin, and the contributions of D. Brodbeck.

27 July 1993; accepted 20 August 1993